

Fermilab

TM-1360
0102.000
(SSC-N-85)

INITIAL ESTIMATE OF TRANSMISSION LINE EFFECTS
IN SSC DESIGN D MAGNETS

O. Calvo and G. Tool

December 1985

Initial Estimate of Transmission Line Effects in SSC Design D Magnets

O. Calvo, G. Tool
December, 1985

Abstract

The response of the SSC accelerator magnet string to transient excitation from the power supply is considered. Some criteria for the selection of the optimum damping resistors for the SSC magnets are discussed. Once the damping resistors are chosen, the transient response of the load to power supply transients, including the effect of the power supply filter is analyzed. A comparative analysis is made of the differences between two possible configurations in the distribution of the magnets (with and without a return bus.)

Introduction

Superconducting magnet strings have electrical properties similar to signal transmission lines. Voltages from the power supply cause 'slow' electrical waves to propagate along the string, resulting in a spatial variation of current in the magnets during the response time. These waves do not typically see a characteristic impedance termination, so reflections add to the original signal, causing a standing-wave pattern of current and voltage in the string. The eddy current losses in the magnets eventually damp this response, but in order to reduce the effect of this response on the accelerator operation to an acceptable level, it is usually necessary to provide some external damping resistance.

Dipole Characteristics

Studies of the electrical characteristics of individual Energy Saver superconducting magnets indicate the circuit shown in Fig. 1 to be appropriate to analyze the transmission line characteristics of the magnets.¹ Since the inductance and eddy current resistance of the coil bus dominates the series impedance, the return bus and ground conductors can be considered to have no resistance or inductance.

1. R. Shafer, "Transmission Line Characteristics of Energy Doubler Dipole Strings", FNAL UPC-37, January, 1979

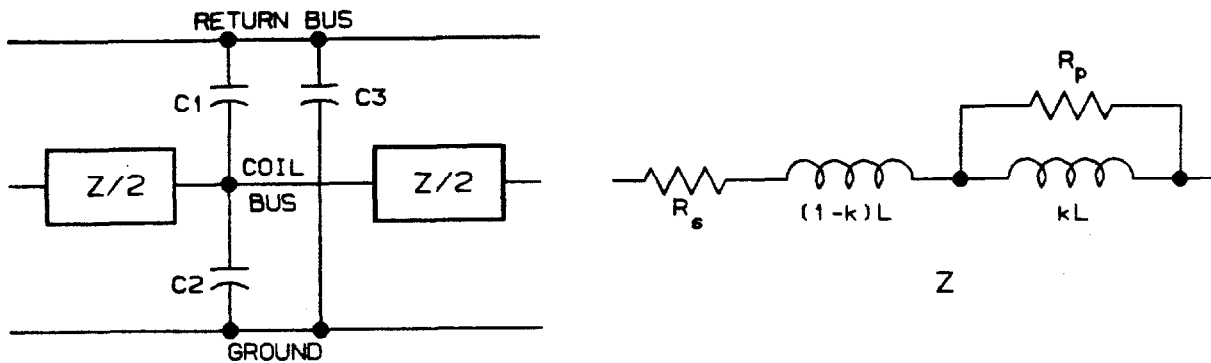


Figure 1. Magnet Equivalent Circuit

In this model,

L = coil inductance

C_i = capacitance between conductors

R_s = coil resistance (0Ω in superconducting state)

R_p = eddy current loss resistance

k = coupling coefficient between L and R_p .

For this analysis, a simpler variation of this circuit shown in Fig. 2 will be used. In Fig. 2, C is the capacitance from coil to ground. C_1 and C_3 of Fig. 1 are estimated to be less than 10% of C_2 and will therefore be ignored.

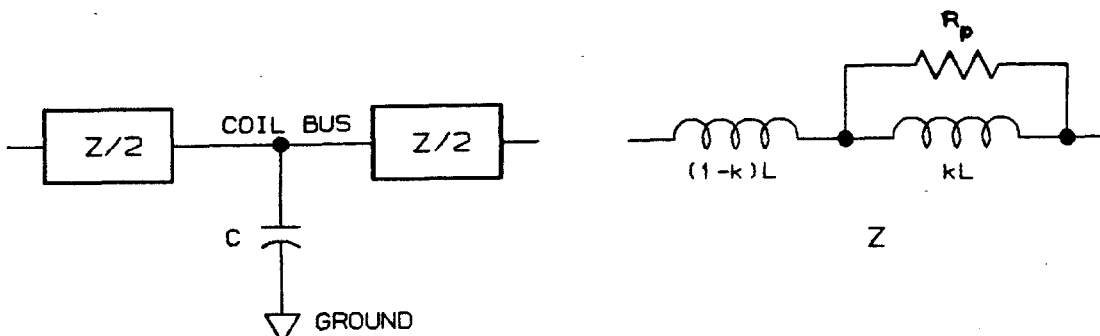


Figure 2. Simplified Equivalent Circuit

From inductance measurements made on early prototypes leading to the present Design D dipole,

$$L' = 3.146 \text{ mH/m}$$

$$l = 16.6 \text{ m/dipole}$$

$$L = (3.146 \text{ mH/m}) * (16.6 \text{ m/dipole}) = 52.2 \text{ mH/dipole}.$$

An estimation of the capacitance per unit length based on measurements of the first 4.5 m SSC magnet prototype is³

$$C' = 4.2 \text{ nF/m.}$$

Then,

$$C = (4.2 \text{ nF/m}) * (16.6 \text{ m/dipole}) = 70 \text{ nF/dipole.}$$

Estimation of Eddy Currents

The eddy current effects in the magnets are strongly dependent on the geometry of the magnets. For the Energy Saver magnets it was shown that the eddy current resistance could be expressed as⁴

$$R_p = kL/\tau$$

where k and τ are determined by the magnet geometry. Until better information is available, the values of these parameters used for the Energy Saver magnet design will be used here to estimate the eddy current resistance for the SSC magnets. These values are

$$k = 0.6$$

$$\tau = 650 \mu\text{s.}$$

Then,

$$R_p = kL/\tau = (0.6) * (52.2 \text{ mH}) / (650 \mu\text{s}) = 48 \Omega.$$

Later knowledge of the mechanical and electrical characteristics of the coils will allow a better estimation of the components of the equivalent circuit. These equivalent circuit components should be verified with direct measurements on the dipoles, once available, to obtain the definitive values. We can make some assumptions in order to obtain preliminary values and then test the sensitivity of the transmission line characteristics to changes made on the equivalent circuit.

Determination of Transmission Line Parameters

With the circuit component values known, we can proceed to characterize the nature of the transmission line circuit formed by a string of dipoles. Design considerations have determined that the power supplies will be situated in the center of the dipole string; the transmission line obtained is shown in Fig. 3 and Fig. 4(a).

3. G. Cottingham, Private Communication, November, 1985

4. R. Shafer, "Eddy Currents, Dispersion Relations, and Transient Effects in Superconducting Magnets", FNAL TM-991, September, 1980

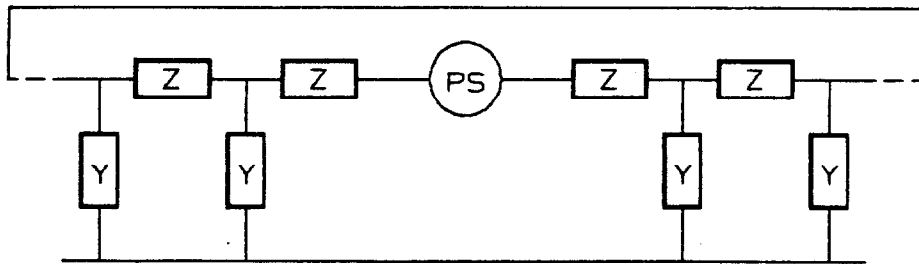


Figure 3. Transmission Line Model of Magnet String

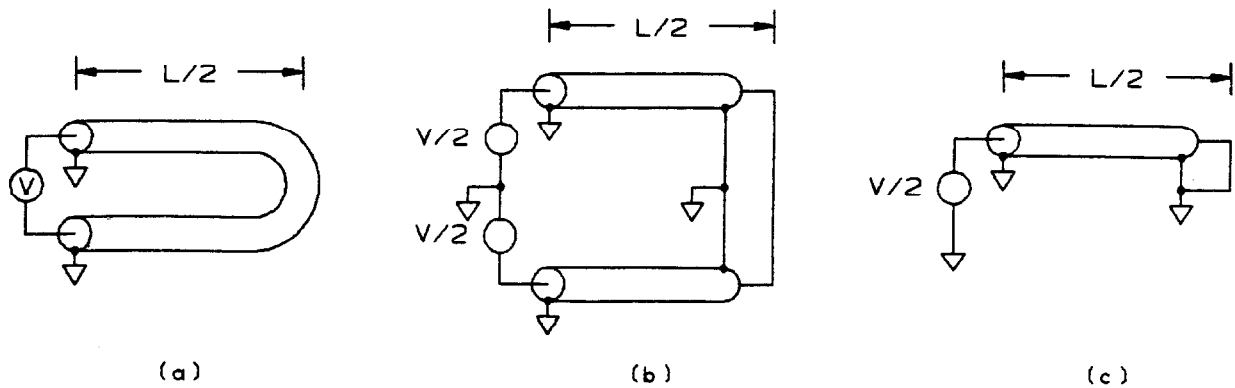


Figure 4. Simplified Transmission Line Model

For purposes of this study, a Design D sector is assumed to contain 80 half-cells of 5 dipoles each, or 400 dipoles total. The contribution of quadrupoles to be connected on the same bus will be ignored as small compared to the dipole contribution. As the line is a homogeneous circuit, the bisection theorem applies, and the load can be split in two symmetrical subcircuits, each 200 dipoles in length as shown in Fig 4(b). Considering the power supply as a pure differential one, the voltage at the end of the subcircuits will be constant and hence, can be considered as ground. Then the analysis can be done considering only one half of the transmission line excited with one half of the power supply and shorted at the end as shown in Fig 4(c). To obtain the overall response, the superposition theorem can be used.

In order to simplify the analytic process to characterize the magnet string as a transmission line, the impedance Z shown in Fig. 2 can be transformed as shown below in Fig. 5.

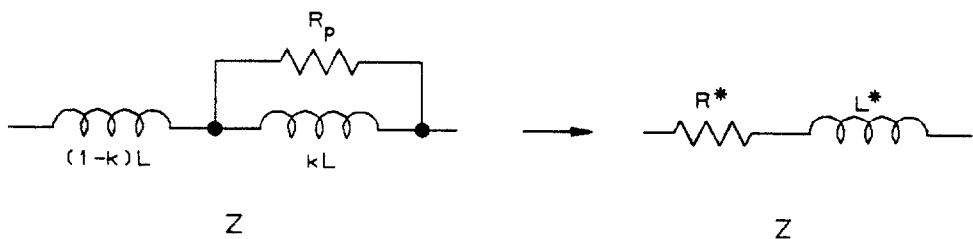


Figure 5. Series Impedance Transformation

$$Z = R^* + j\omega L^*$$

$$R^* = \frac{kL\tau\omega^2}{1 + \omega^2\tau^2}, \quad L^* = (1-k)L + \frac{kL}{1 + \omega^2\tau^2}, \quad \tau = \frac{kL}{R_p}$$

Both R^* and L^* are functions of ω .

The differential equations of the transmission line are:

$$\frac{de(x,t)}{dx} = -R^*i(x,t) - L^* \frac{di(x,t)}{dt}$$

$$\frac{di(x,t)}{dx} = -C \frac{de(x,t)}{dt}$$

The steady state sinusoidal solution of these equations of the form $e^{j\beta x}$ considering a line with a short circuit at $x = 0$ leads to an impedance

$$Z(x) = \frac{e(x)}{i(x)} = Z_0 \frac{e^{\gamma x} - e^{-\gamma x}}{e^{\gamma x} + e^{-\gamma x}}$$

$$Z_0 = \sqrt{\frac{Z(\omega)}{Y(\omega)}}$$

$$\gamma = \alpha + j\beta = \sqrt{|Z(\omega) \cdot Y(\omega)|}$$

The propagation velocity is:

$$v_p = \omega/\beta$$

The attenuation length is given by:

$$\lambda = 1/\alpha$$

These equations can be simplified to analyze the low frequency behaviour of the magnet string to

$$Z_0 \approx \sqrt{L^*/C}$$

$$v_p \approx \sqrt{1/L^*C}$$

$$\lambda \approx \frac{2Z_0}{R^*(\omega)} \text{ magnets to } 1/e.$$

Standing waves will exist at frequencies:

$$f_n = nv_p/N$$

and

$$Q_n = w_n L^*(w_n)/R^*(w_n)$$

where:

n = odd or even number half integer

N = number of magnets in the total string.

Application to SSC Magnets

Using the simplified equations and the SSC Design D parameters we obtain:

$$Z_0 = 861 \Omega$$

$$v_p = 16565 \text{ dipoles/s}$$

$$f = 41.4 \text{ Hz}$$

$$T = 24.1 \text{ ms}$$

$$Q = 10.2$$

where f , T and Q are for the half-wave resonance.

An SCR power supply usually has ripple output at power line harmonic frequencies, with the 120 Hz component often predominate because of power line unbalance and difficulty in filtering at this frequency. Hence it is important to know the value of the attenuation length and the quality factor Q at this frequency.

$$L^*(120 \text{ Hz}) = 46.13 \text{ mH}$$

$$R^*(120 \text{ Hz}) = 9.33 \Omega$$

$$\lambda_{120 \text{ Hz}} = 175 \text{ dipoles to } 1/e \text{ of the value at } x = 0$$

$$Q_{120 \text{ Hz}} = 3.7$$

In order to decrease the effect of power supply ripple and to obtain a desirable transient response to voltage steps from the power supply, an external damping mechanism must be included. The solution adopted for the Energy Saver seems to be applicable in this case. A damping resistor will be placed in parallel with a half cell or cell of magnets. As in the Energy Saver, the value will be determined by minimizing the attenuation length at a specific frequency of interest.

Selection of the Optimum Damping Resistor

A Fortran program was used to calculate the transmission line properties of the Design D magnet string as a function of the damping resistor, R_d . The results for 41.4 Hz (half-wave resonance, curve A) and 120 Hz (curve B) are shown in the graph of Fig. 6. For 41.4 Hz, it can be seen that the attenuation length has a minimum value for a resistance of 8.25 Ω , and for 120 Hz it can be seen that the attenuation length has a minimum value for a resistance of 25.5 Ω per dipole.

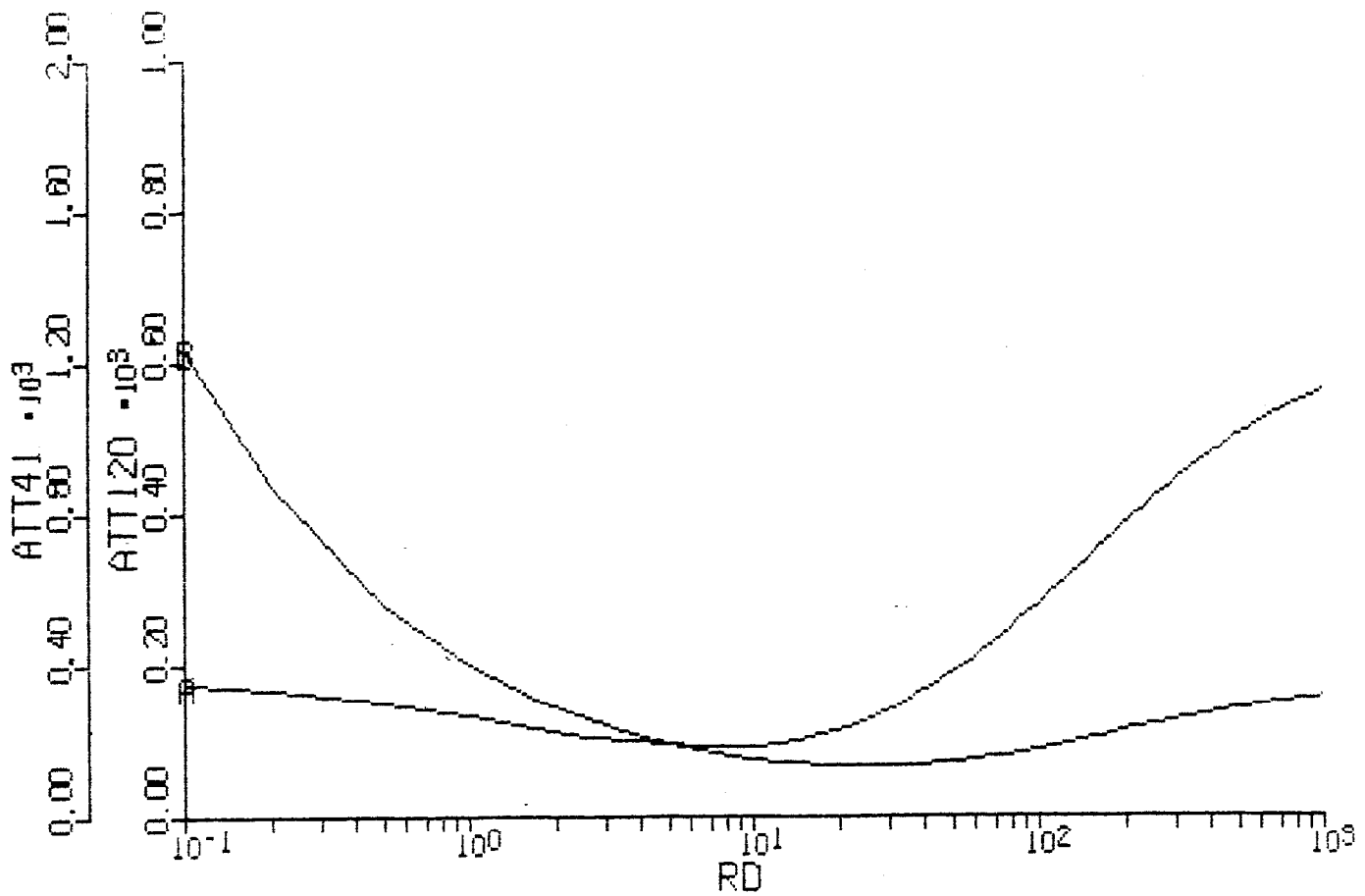


Figure 6. Attenuation Length (λ) vs. Damping Resistance

For the 120 Hz optimum damping resistor, the time constant of the dipole magnets is

$$TC = L/R_d = 2 \text{ ms.}$$

This value is very close to the one obtained for the Energy Saver (2.3 ms). Once a damping resistor value is chosen, it is valuable to analyze the results of the transmission line equations for different frequencies. Table I below summarizes these values for important frequencies for the three damping resistor cases mentioned above.

F (Hz)	5	41.4	120	720	1440
--------	---	------	-----	-----	------

For no external damping resistor:

λ (dipoles)	85487.4	1273.3	174.7	27.7	23.9
v_p (dip./s)	16535.4	16653.4	17440.9	23893.8	25444.9
Z_0 (Ω)	863.0	857.9	825.3	608.0	564.7
Z_I (Ω)	689.3	269.0	1646.1	1216.0	1129.4
Q	81.2	9.9	3.7	2.5	4.2

For a 25.5 Ω damping resistor:

λ	13791.8	250.1	63.7	18.3	12.1
v_p	16570.8	18770.2	27734.2	68538.8	96869.0
Z_0	861.7	791.2	594.0	270.6	197.0
Z_I	687.2	1178.3	1188.6	541.1	394.0
Q	13.1	1.6	0.6	0.2	0.1

For a 8.25 Ω damping resistor:

λ	5125.3	180.4	79.0	29.0	20.1
v_p	16806.4	27117.5	48414.3	122977.3	174419.8
Z_0	853.7	607.8	379.8	159.1	113.5
Z_I	673.0	1436.1	750.0	318.2	227.0
Q	4.7	0.6	0.2	0.1	<0.1

Table I. Transmission Line Parameters

These results show that for the low frequency domain Z_0 and v_p match the values previously calculated with the approximate equations. It should be noted that as the line doesn't meet the distortionless condition, the velocity of propagation is strongly dependent on frequency; for that reason we can't define a delay for a signal travelling along the line, unless it has only one frequency component. The input impedance of the line (Z_I in above tables) in the high frequency domain is twice the characteristic impedance Z_0 ; this ratio is independent of frequency and the damping resistor.

In order to analyze the sensitivity of the value of the damping resistor to the eddy current resistance R_d , a case was calculated considering this resistance to be infinite (no loss). The 120 Hz optimum value for the damping resistor in this case is 22.4 Ω , which indicates that the eddy current model chosen does not greatly affect the selection of R_d . The low resistance of the optimum R_d attenuates the sensitivity to changes in R_d .

The strong influence of the damping resistor on the attenuation of the travelling wave can be seen. When the damping resistor was changed from 25.5 Ω to 8.25 Ω , the attenuation length at the 41.4 Hz resonance changed from 250 dipoles to 180 dipoles which means a shorter settling time and less overshoot. From the table it can also be seen that the attenuation length for 120 Hz ripple increases from 64 to 79 dipoles, a small increase.

The optimum value for an actual design is probably somewhere in the range of these two values. One has to trade off the damping performance desired with power dissipation and shunt current effects when the actual ramping voltage to be used is better known. For a ramping condition as indicated in the SSC Reference Design Study, a voltage of 100 V from the power supply leads to power dissipations and shunt currents as indicated in Table II below for the two values of damping resistance studied above. For these conditions, it is clear that the power dissipation in the damping resistors due to ramping is of no concern.

<u>Damping Resistor</u>	<u>Total Sector Power</u>	<u>Shunt Current</u>
25.5 Ω	1 W	11 mA
8.25 Ω	3 W	30 mA

Table II. Damping Resistor Power and Shunt Current

The magnet string could be considered as a second order filter, with a half-wave resonant frequency of 41.4 Hz where the higher resonances are not important because of the strong drop of the attenuation length with frequency.

Computer Simulation of the Magnet String Response

In order to provide further insight into the behaviour of the magnet string, a SPICE⁶ model of approximately one sector of Design D magnets containing 16 subcircuits of 25 dipoles each has been generated as shown in Fig. 7. A magnet equivalent circuit based on Fig. 2, shown in the center of Fig. 7, including an eddy current resistance was used. The dependent current generators designated F0 - F8 in the schematic provide a method for summing the effect of the current in the two magnet busses at the location just below each generator, i.e., the current in F1 is the average of the two currents flowing in the 'ammeters' V6 and V8. This is useful for evaluating configurations in which the magnetic field is due to the sum of the currents in the two busses.

A SPICE ac analysis was conducted for the magnet string with no damping resistor and each of the two damping resistor values discussed above. The input impedance plots for these cases shown in Fig. 8, Fig. 9, and Fig. 10 show the lowest frequency resonances of the magnet string model and how they are affected by the damping resistance. The half-wave 41.4 Hz resonance calculated for the simplified transmission line model is verified in the impedance plot of Fig. 8.

To study the system response to voltage transients from the power supply, a differential perturbation of the voltage of

6. SPICE is a general purpose circuit simulation program developed by the Department of Electrical Engineering and Computer Sciences at University of California, Berkeley and used throughout the electronics industry.

approximately 10% full output with rise and fall times appropriate for a 12-pulse SCR controlled power supply was used. Transients of this nature should be expected in a real system of this type. To model a realistic situation and include the effects of the output filter of the power supply on the transient response, a second order low pass filter plus a trap centered at 720 Hz was included. The filter modelled in this case is the same as that used in the Energy Saver.

Cases were studied for no damping and for the two values of damping resistance. Since we do not know what actual coil and bus configuration is to be used, we analyzed two cases:

- 1.) A global return bus system in which all inductance is on the bus connected to the power supply terminals with a stabilized return bus outside the magnetic field running the total length of the sector. (In this case, nodes 2 and 171 of the circuit diagram (Fig. 7) represent this return bus circuit, and nodes 81 and 90 represent the half-way points along each half-sector.)
- 2.) A "split-bus" system in which half of the inductance is on each of two busses (either as in one of H. Edwards variations of SSC magnet design,⁷ or with alternations of coils and return busses as in the Energy Saver) assuming that the effective current contributing to the magnetic field is the sum of the currents in the two busses. This case has been analyzed with and without magnetic coupling between the two busses. Fig. 11 shows the input impedance with this magnetic coupling included for the case of no damping resistance to be compared to Fig. 8. Note that the half-wave resonant frequency is doubled when magnetic coupling is added.

The split-bus case shows an interesting compensation effect, i.e., the sum of the magnet currents in the two busses varies less with distance from the power supply. How practical this effect is depends on the viability of a split-bus magnet design or whether the effect on the beam can be integrated over several magnets with their coils distributed between the two busses.

The transient response of the magnet string for these cases is displayed in Fig. 12 - Fig. 18. The conditions of the analysis and the definitions of the various symbols on the graphs are given in the heading material in each figure. Time is expressed in seconds, and current in amperes.

Although there is significant difference in the ac input impedance when magnetic coupling between the two busses is included, no significant difference in effective magnetic field transient response from the uncoupled case was noted for the split-bus model with magnetic coupling added.

The figures show that the overshoot, the signal delay, and the maximum current difference through the magnet system are reduced by the addition of the external damping resistor. For

the transient studied, the delay, maximum overshoot, and maximum instantaneous difference in current between any two locations in the magnets are summarized in Table III below.

	<u>Global Return Bus</u>			<u>Split Bus</u>		
R_d (Ω)	*	25.5	8.25	*	25.5	8.25
Delay (μs/dip.)	30	26	21	15	13	9
Overshoot (%)	264	117	61	100	56	39
ΔI (mA)	13.9	8.2	4.1	5.4	2.4	1.1

Table III. Transient Response Summary

Impact on Power Supply Regulation

In addition to the effects noted above, addition of damping resistors to the magnet string has a significant effect on the behaviour of the power supply current regulation system. From the SPICE ac analysis results in Fig. 8 - Fig. 10, it is apparent that the damping resistor value has a significant effect on the magnitude and phase of the input impedance of the load. Since a lower value of damping resistance results in a smoother function, it would appear that a regulator would have greater stability with this load than with one which exhibits alternating peaks in impedance. A closed-loop analysis of regulator stability should be conducted to determine if an optimum damping resistor value can be chosen from this consideration.

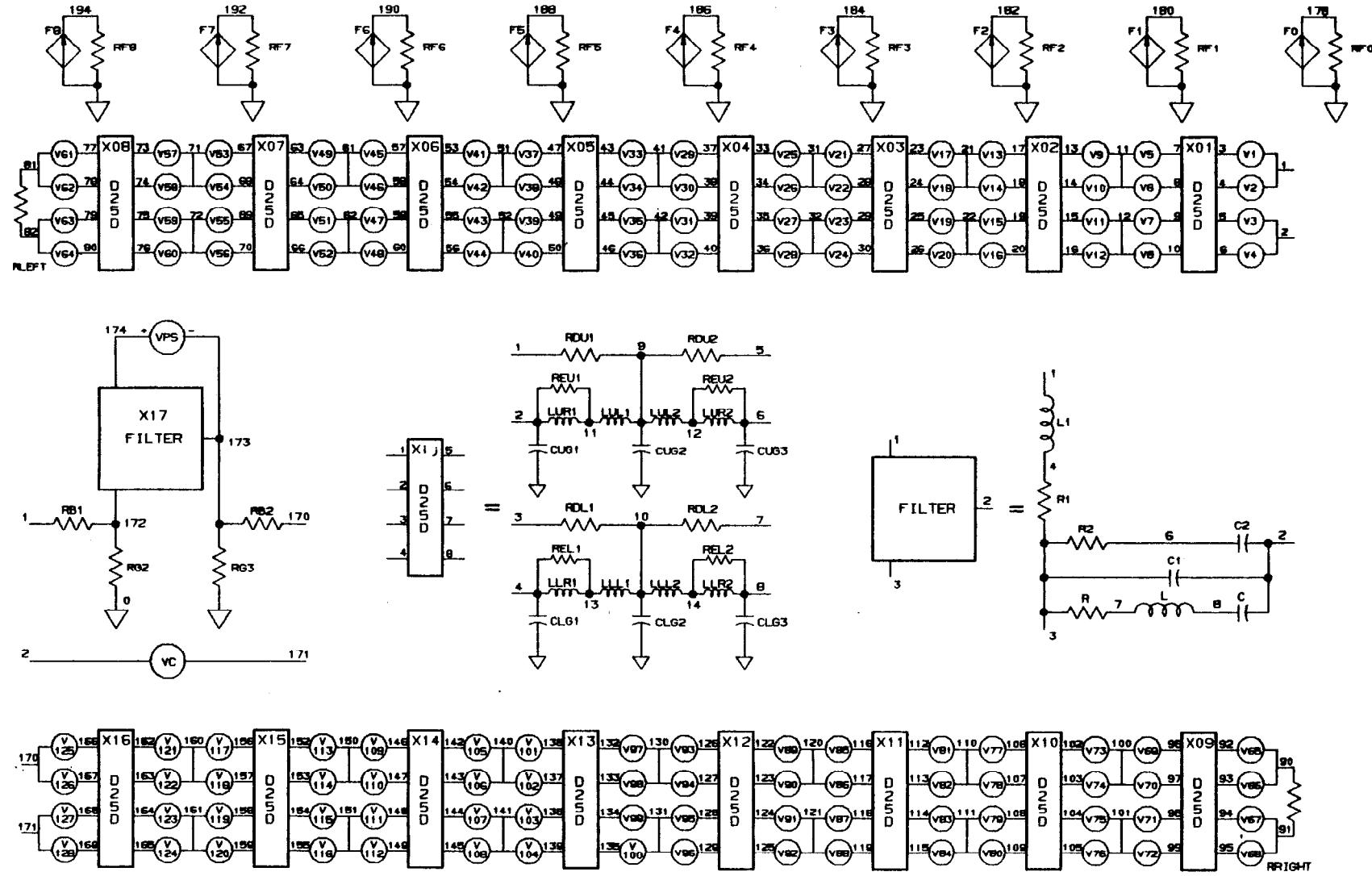
Conclusions

This first analysis of the transmission line behaviour of the SSC magnet string using Design D magnets does not indicate any serious problems to be expected in the system electrical behaviour. It does indicate however that external damping resistors should be added to the magnet string to reduce the effect of power supply ripple and to reduce the magnetic field spatial distortions due to power supply transients. The value of resistance used is not critical and with the ramping voltages expected in the SSC, the power dissipation in these resistors is negligible. The power rating of the resistors may be determined from other considerations such as the voltage due to dumping the energy from the system during a quench.

A significant difference in transmission line behaviour of the magnet system has been noted dependent on the distribution of the magnet coil windings on the two busses passing around the ring. Splitting the coil windings on two busses rather than having them all on one bus with the other bus acting as a return bus outside the magnetic field appears to have a beneficial effect on the electrical behaviour of the circuit.

No attempt has been made to evaluate the effect of the calculated current distributions due to transients or the shunt current through the damping resistors during ramping on the magnetic field and hence the accelerator beam. The results presented here may be useful to others for this purpose.

Figure 7. SPICE Model Schematic



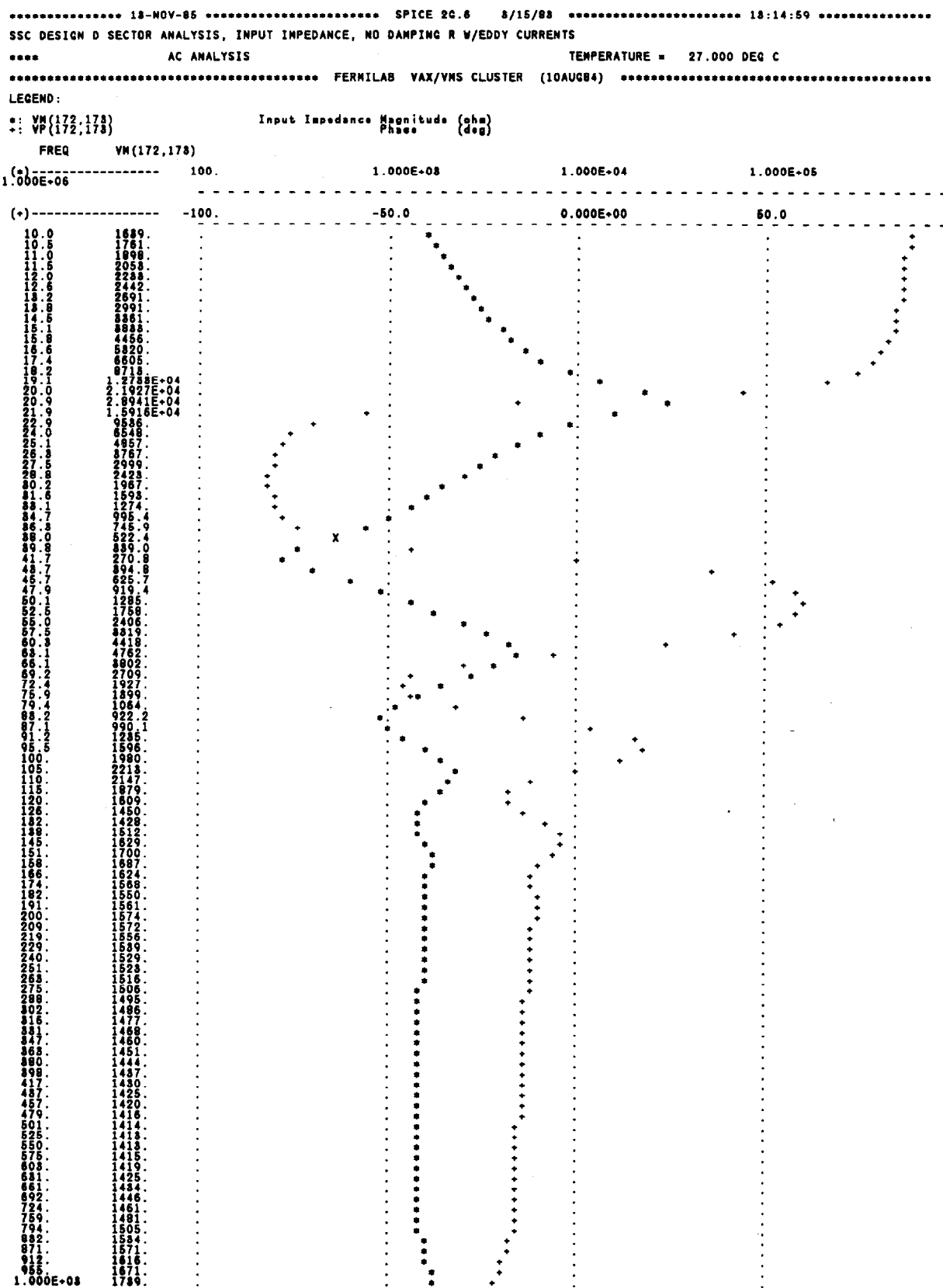


Figure 8. Input Impedance With No Damping Resistor

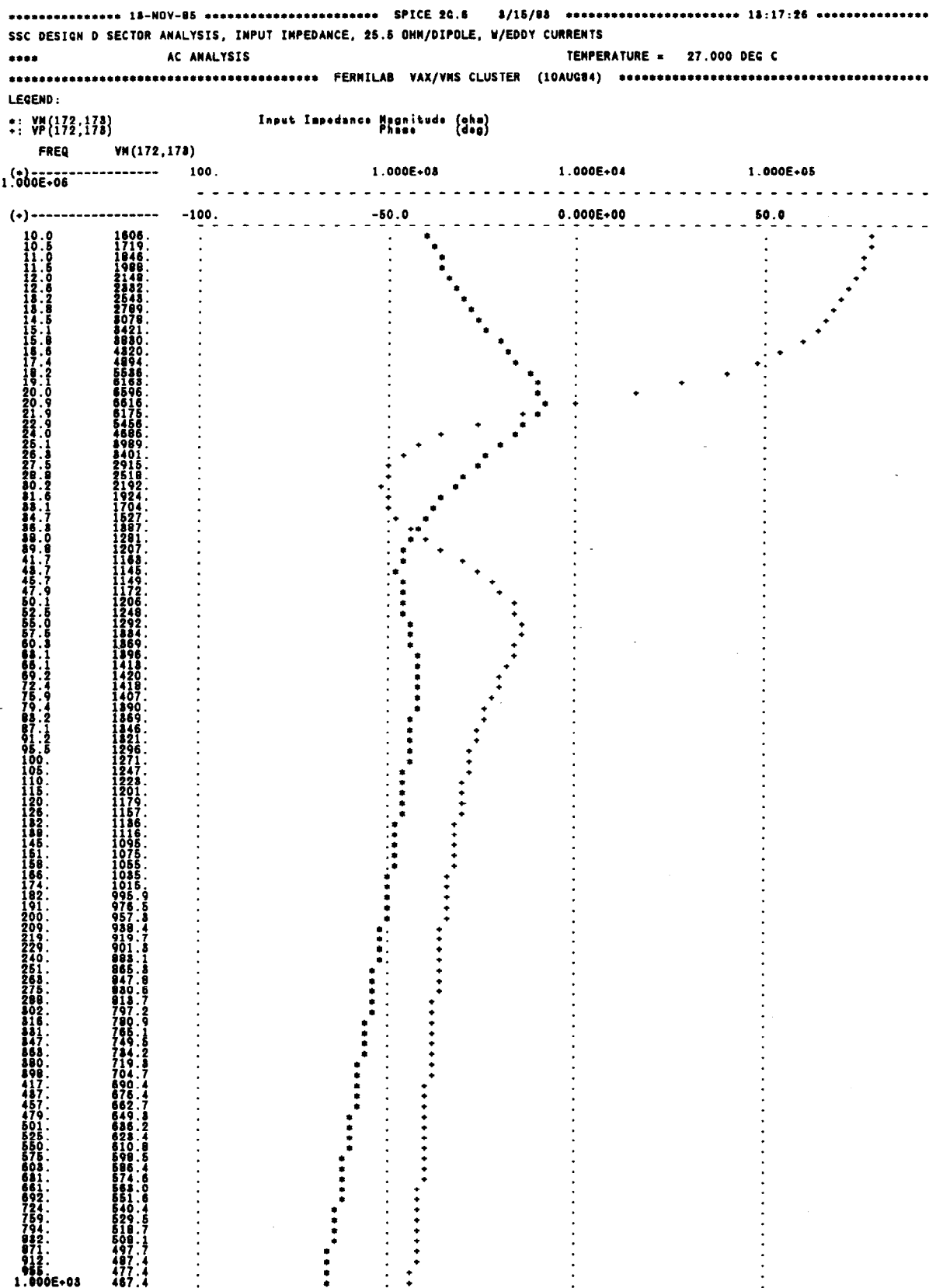


Figure 9. Input Impedance With 25.5 Ω Damping Resistor

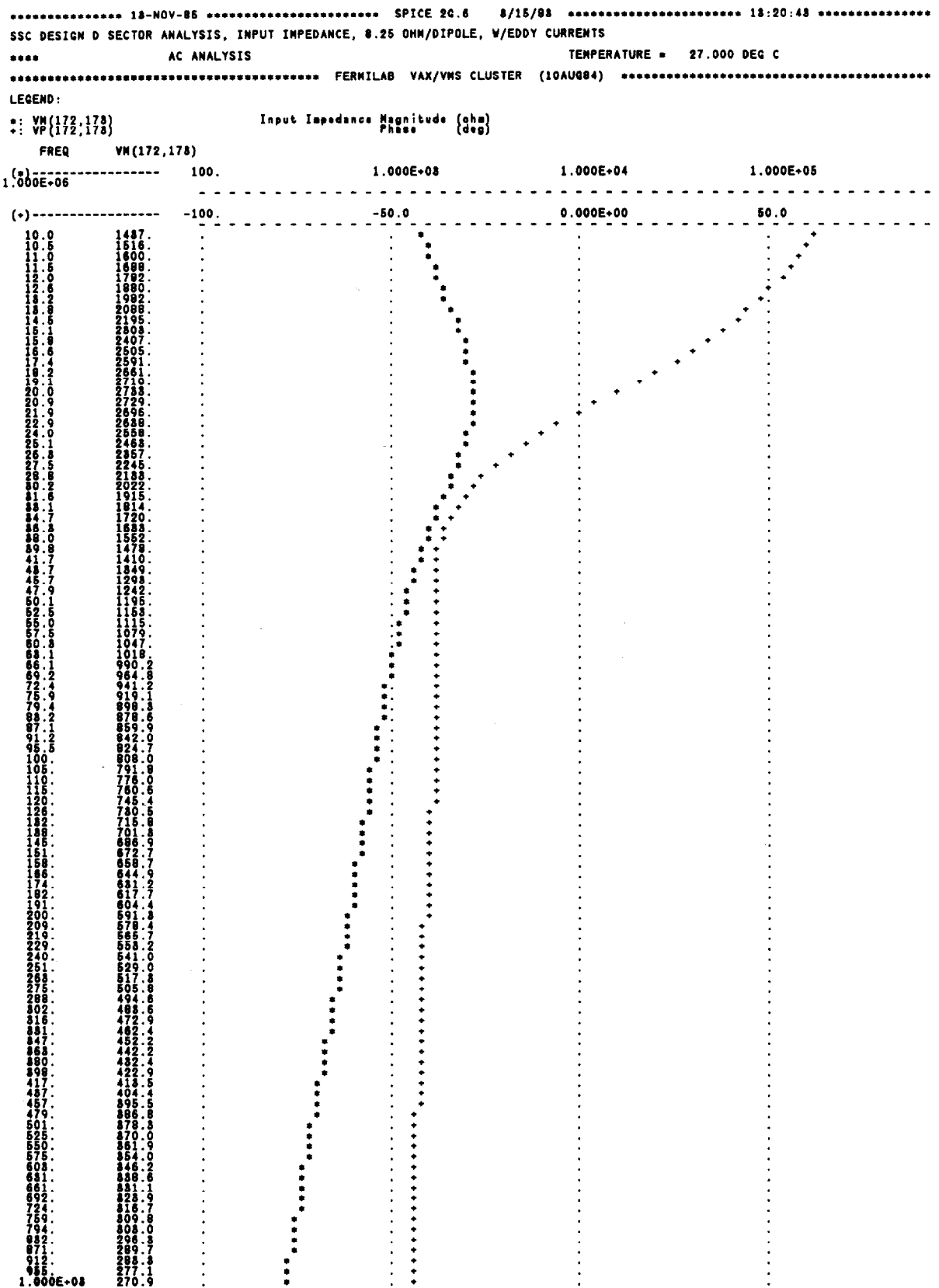


Figure 10. Input Impedance With 8.25 Ω Damping Resistor

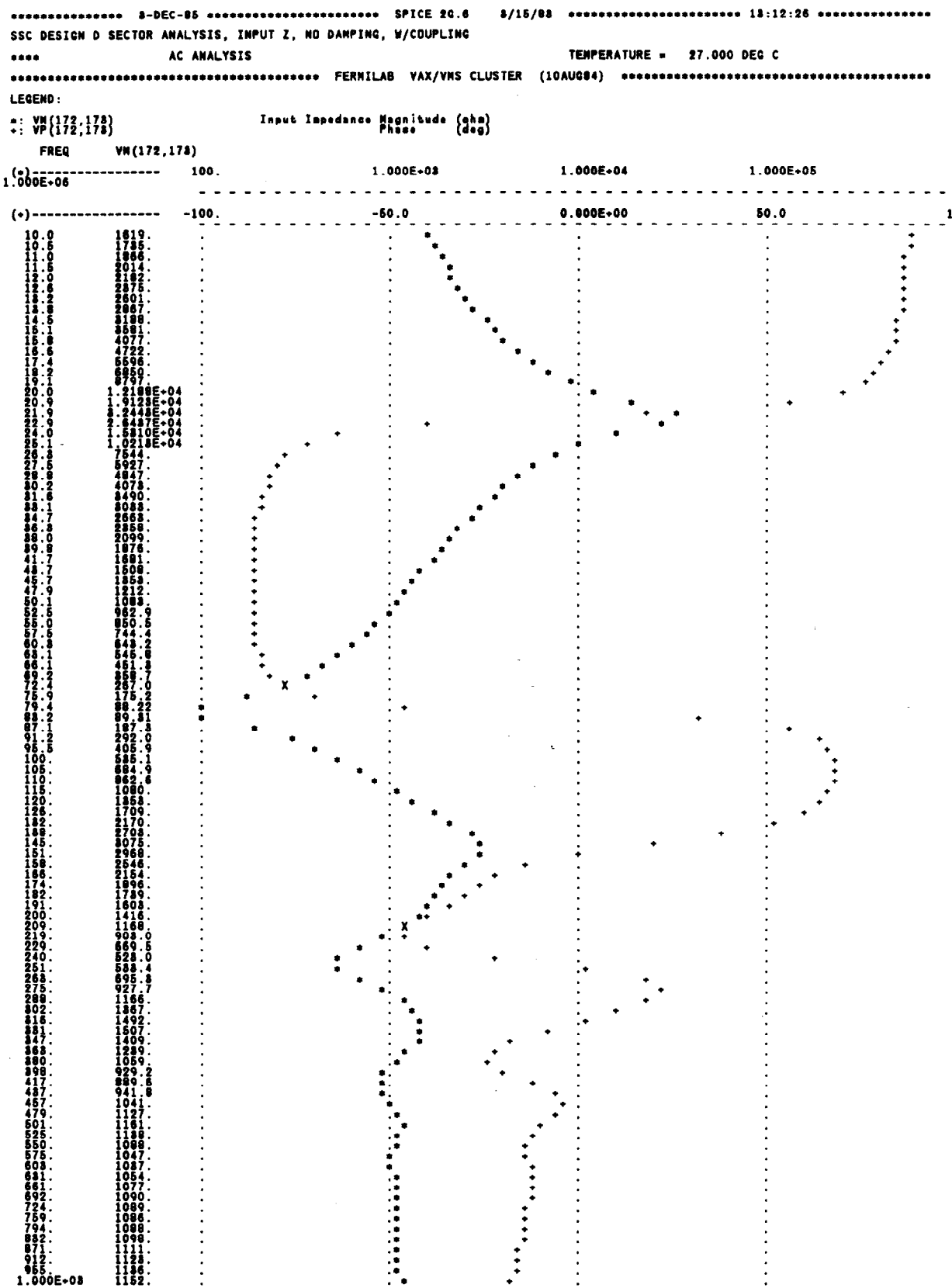


Figure 11. Input Impedance With Magnetic Coupling, No Damping

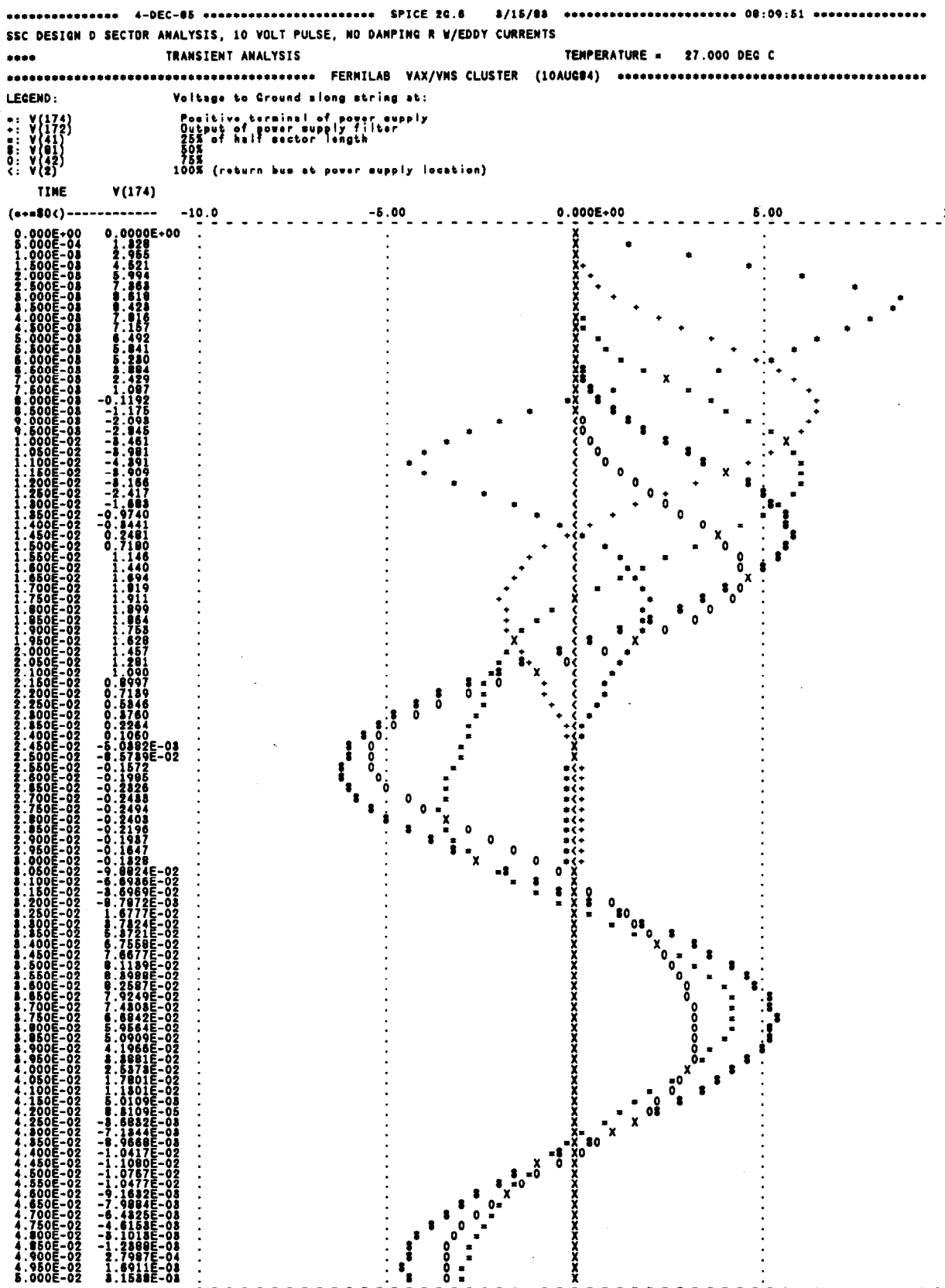


Figure 12. Transient Voltage Along String

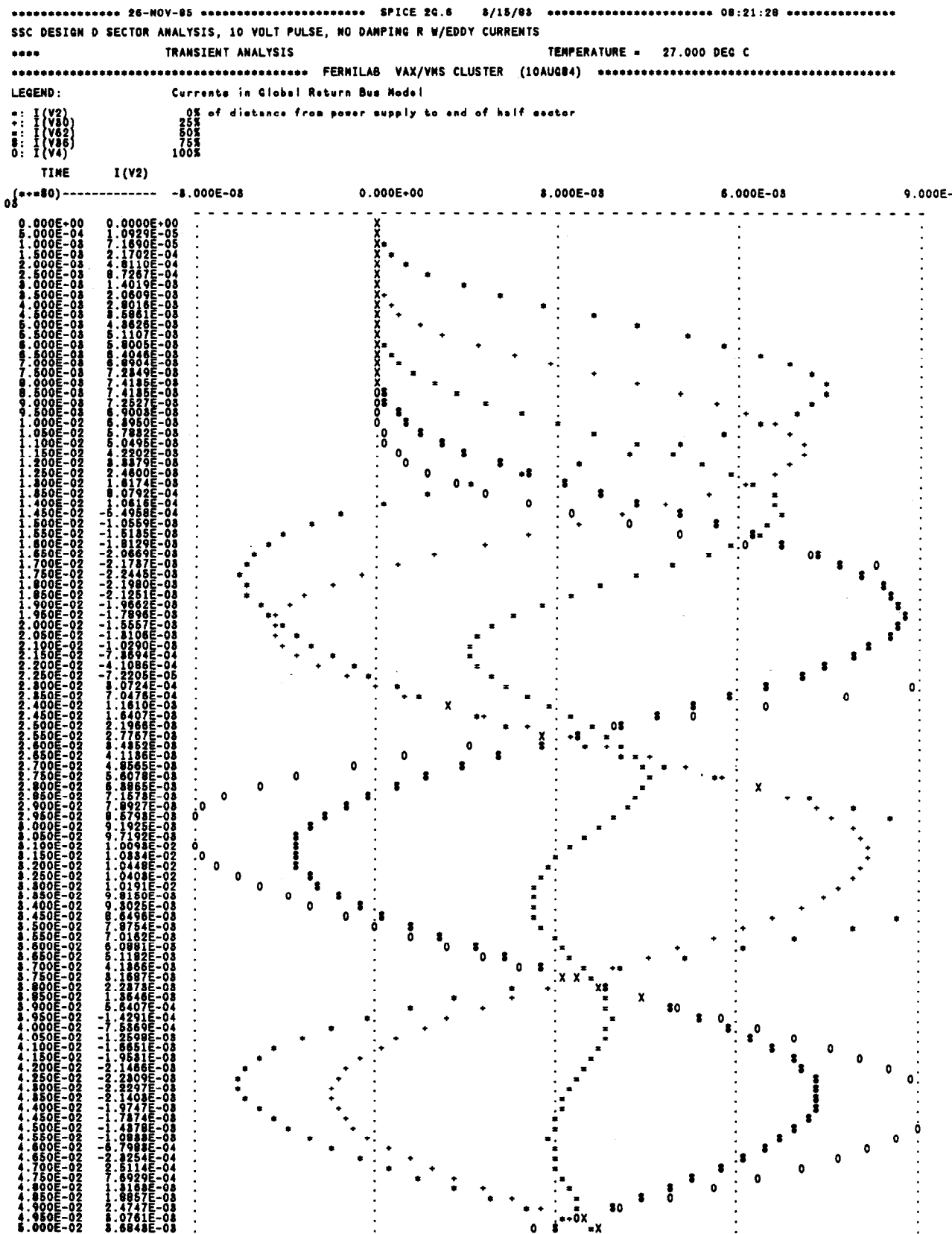


Figure 13. Transient Response, No Damping, Return Bus Model

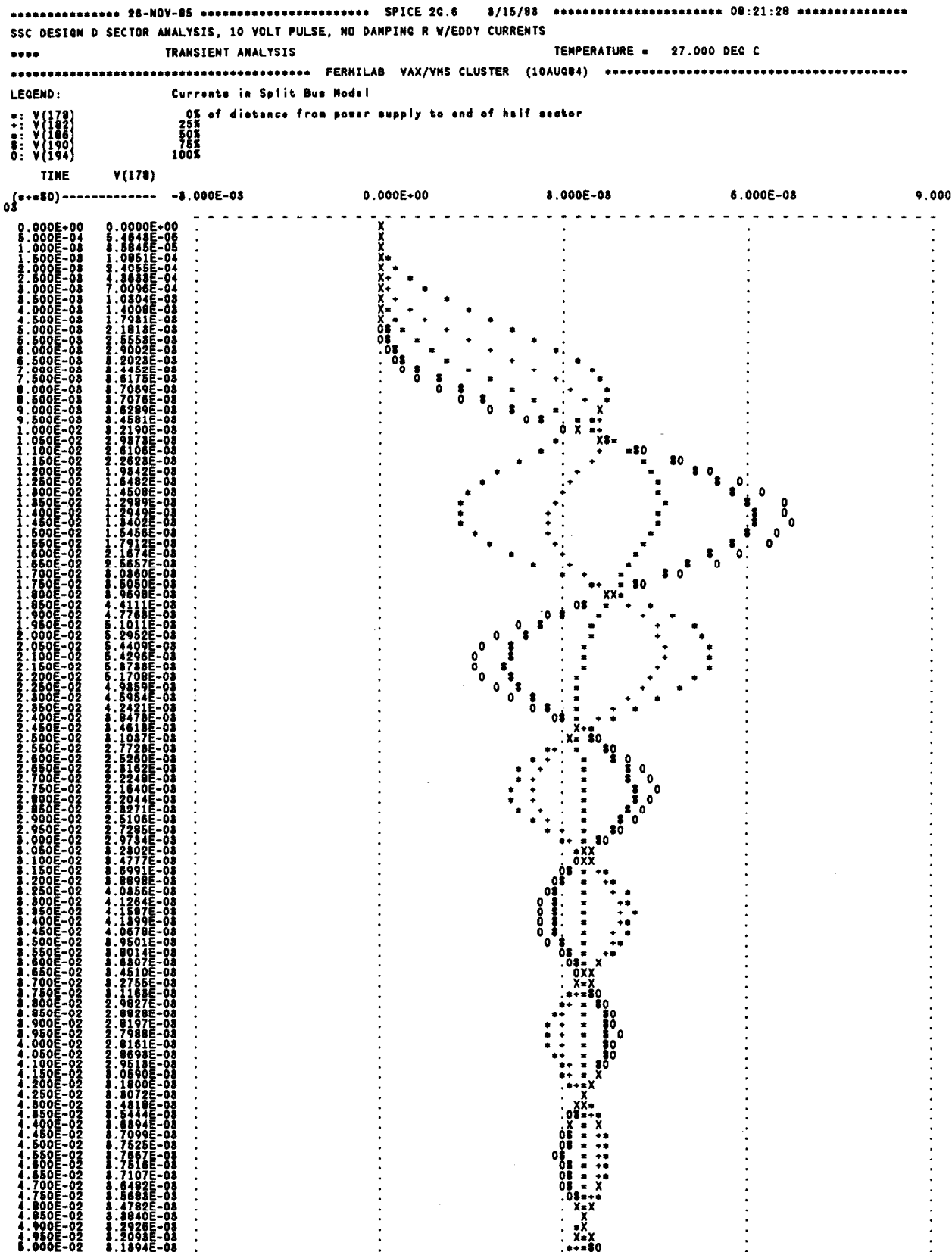


Figure 14. Transient Response, No Damping, Split Bus Model

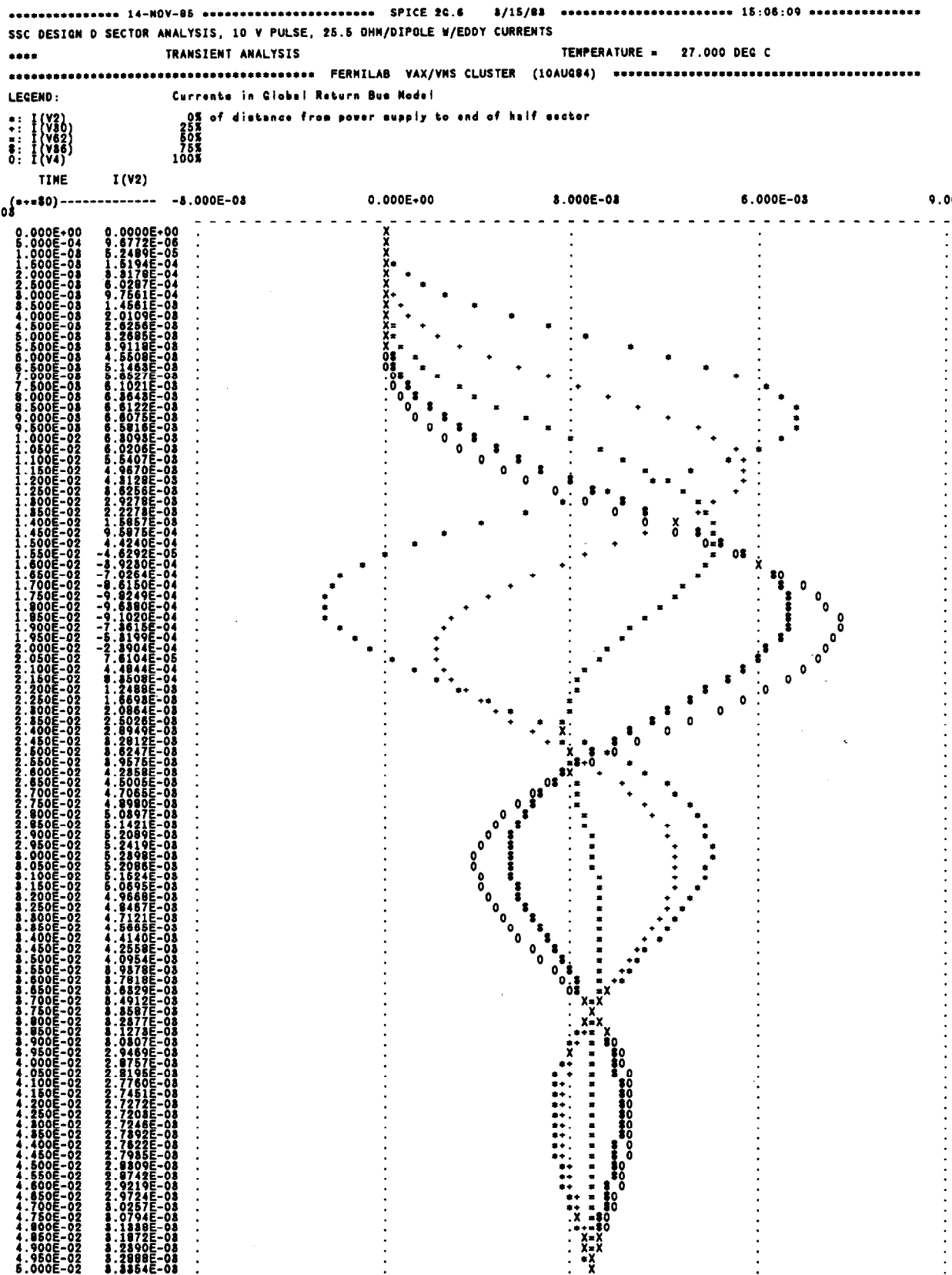


Figure 15. Transient Response, $R_d = 25.5 \Omega$, Return Bus Model

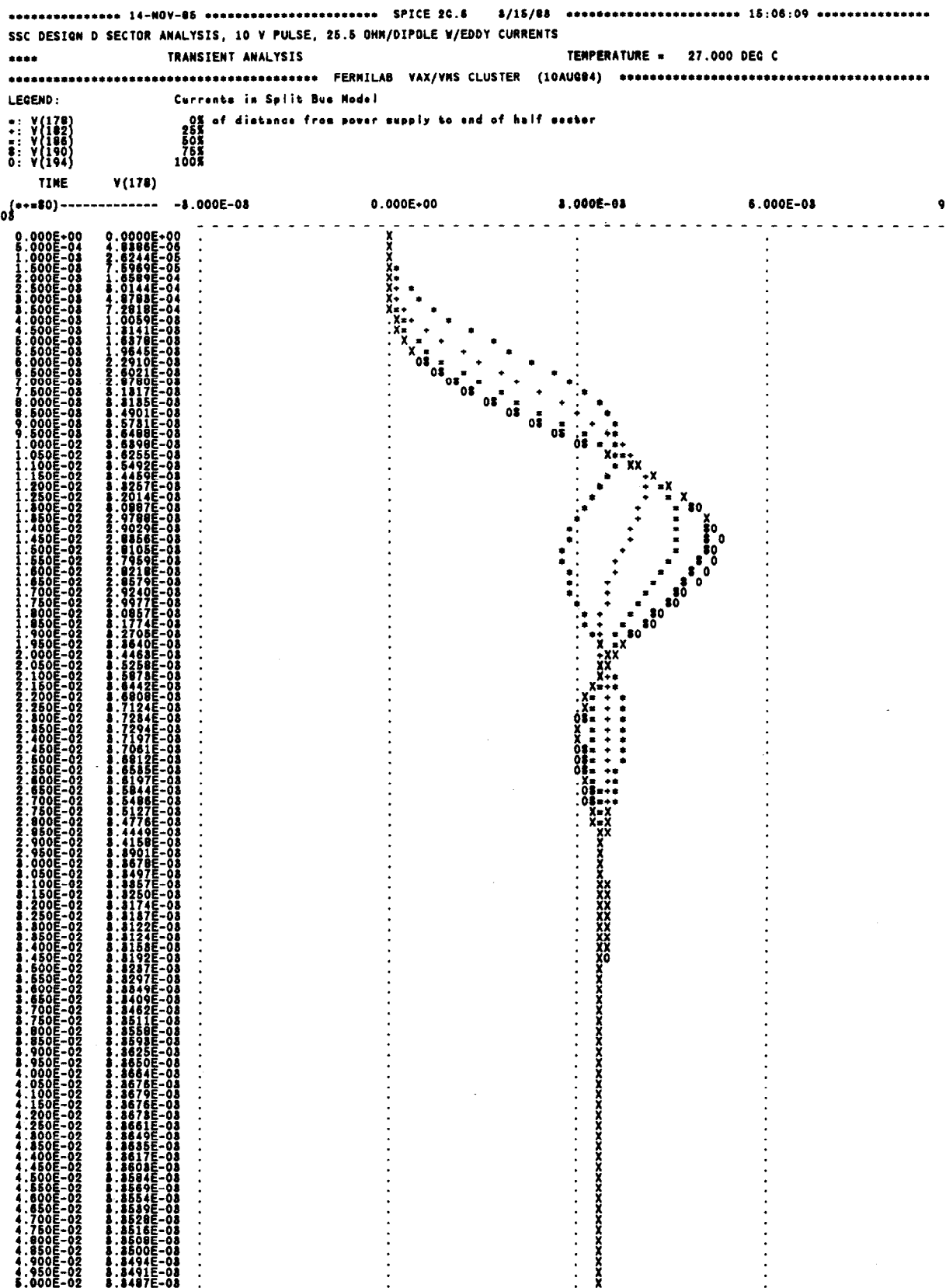


Figure 16. Transient Response, $R_d = 25.5 \Omega$, Split Bus Model

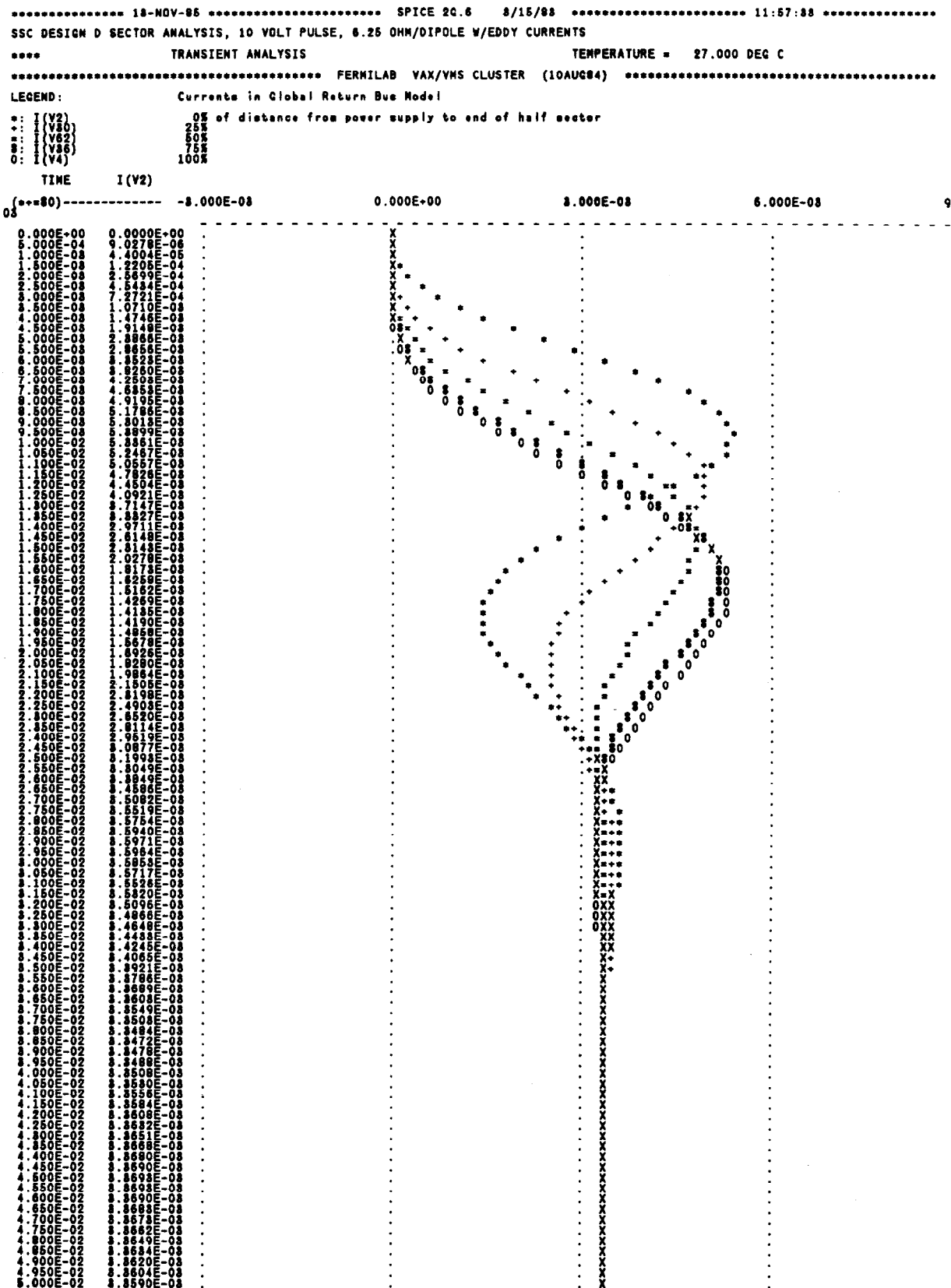


Figure 17. Transient Response, $R_d = 8.25 \Omega$, Return Bus Model

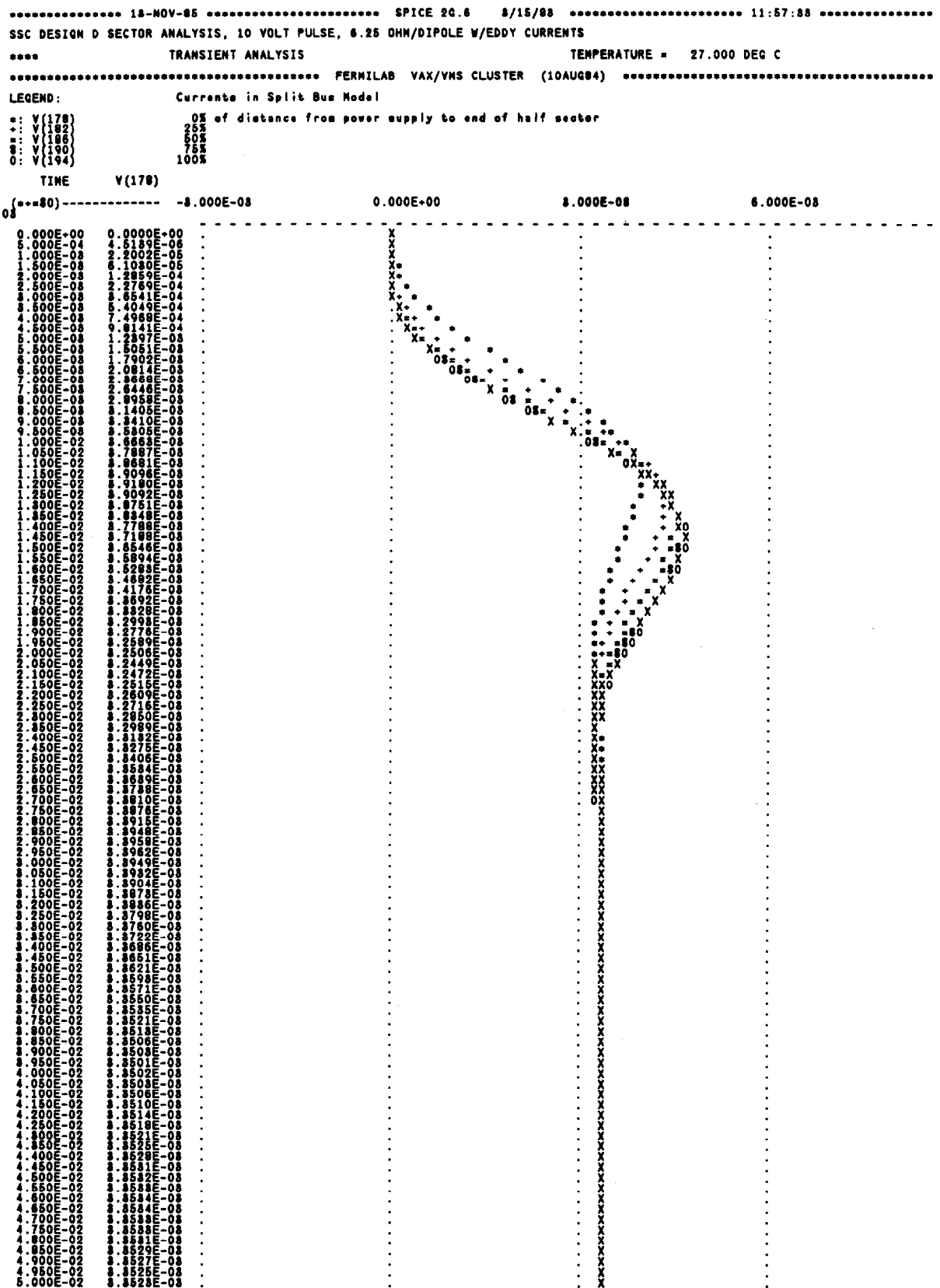


Figure 18. Transient Response, $R_d = 8.25 \Omega$, Split Bus Model